

Improving Bracket Image Restoration and Enhancement with Flow-guided Alignment and Enhanced Feature Aggregation

Wenjie Lin¹ Zhen Liu¹ Chengzhi Jiang¹ Mingyan Han¹
 Ting Jiang¹ Shuaicheng Liu^{2,1†}

¹Megvii Technology ²University of Electronic Science and Technology of China
<https://github.com/NygmaLin/IREANet>

Abstract

In this paper, we address the Bracket Image Restoration and Enhancement (BracketIRE) task using a novel framework, which requires restoring a high-quality high dynamic range (HDR) image from a sequence of noisy, blurred, and low dynamic range (LDR) multi-exposure RAW inputs. To overcome this challenge, we present the IREANet, which improves the multiple exposure alignment and aggregation with a Flow-guide Feature Alignment Module (FFAM) and an Enhanced Feature Aggregation Module (EFAM). Specifically, the proposed FFAM incorporates the inter-frame optical flow as guidance to facilitate the deformable alignment and spatial attention modules for better feature alignment. The EFAM further employs the proposed Enhanced Residual Block (ERB) as a foundational component, wherein a unidirectional recurrent network aggregates the aligned temporal features to better reconstruct the results. To improve model generalization and performance, we additionally employ the Bayer preserving augmentation (BayerAug) strategy to augment the multi-exposure RAW inputs. Our experimental evaluations demonstrate that the proposed IREANet shows state-of-the-art performance compared with previous methods.

1. Introduction

Image restoration and enhancement (IRE), which aims to obtain high-quality image results from single or multiple degraded images, is a fundamental yet still challenging low-level vision problem. Compared to single-image restoration and enhancement [13, 16, 21, 27, 41–43, 46], utilizing multi-frame information to solve these ill-posed problems is more practical and has shown greater potential [5, 11, 29, 36].

Existing multi-frame IRE methods can be broadly divided into two categories: BurstIRE and Multi-exposure IRE. BurstIRE methods exploit multiple consecutive frames

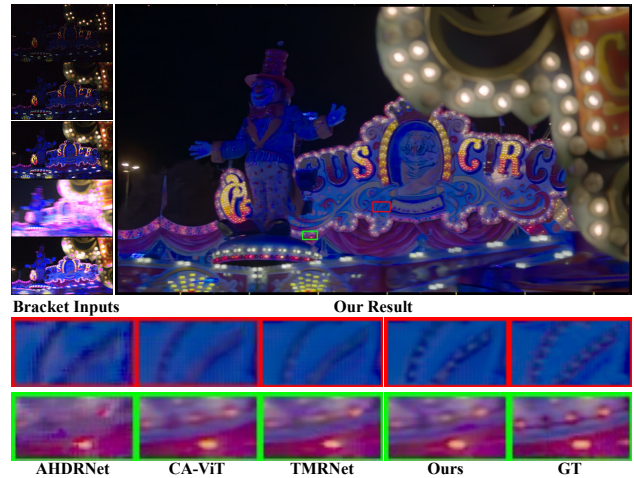


Figure 1. Comparisons between the proposed IREANet and other representative methods [23, 40, 44]. Our result is free of noise and blur while producing more details.

of images with identical exposure to tackle tasks like denoising, deblurring, and high dynamic range (HDR) imaging. For instance, burst denoising [14, 26, 32, 39] leverages a burst capture of short-exposure to predict a single noise-free and unblurred image estimate by considering the fact that noise is independent across different frames. Burst deblurring [1, 10, 37] aggregates a burst of inputs into a single image that is both sharper and less noisy than all the images in the burst. Techniques like HDR+ [15] utilize raw bursts for more practical HDR reconstruction on commercial smartphones.

However, the limited scene information of burst inputs, e.g., dynamic range and noise level, hinders the further development of BurstIRE. Conversely, by benefiting from a wider dynamic range and richer levels of noise and motion blur across different exposures, Multi-exposure IRE has recently received more attention for being more efficient and practical in tasks such as HDR reconstruc-

tion [17, 22, 23, 28, 38, 40] and denoising [9, 20]. Motivated by the complementary nature of multi-exposure images in denoising, deblurring, and HDR reconstruction, the NTIRE2024 (New Trends in Image Restoration and Enhancement) introduced the BracketIRE challenge [45], which aims to jointly perform denoising, deblurring, and HDR reconstruction tasks by utilizing multi-exposure images.

In this paper, we propose the IREANet, which improves the feature alignment and feature aggregation in the BracketIRE task. Specifically, the proposed IREANet mainly comprises a flow-guided feature alignment module (FFAM) and an enhanced feature aggregation module (EFAM). The proposed FFAM employs the optical flow between bracket exposures to guide the optimization of the deformable alignment and the spatial attention, enabling more effective alignment of the bracket inputs. Moreover, to enhance the stability and efficiency of the feature aggregation, we propose an Enhanced Residual Block (ERB), which enhances the nonlinearity of the vanilla residual block by adding a 1×1 convolutional layer and a nonlinear activation layer. Through the incorporation of the proposed ERB as the foundational module, the EFAM achieves better convergence, thereby allowing for efficient aggregation of temporal features. Additionally, to preserve the correct Bayer pattern of the RAW images, we adopt a Bayer preserve augmentation (BayerAug) strategy to eliminate the issues of Bayer misalignment in the training data during augmentation. Based on the aforementioned components, the proposed IREANet is capable of producing visually pleasing, high-quality HDR results with clear content and enhanced details (as illustrated in Fig. 1).

Our main contributions can be summarized as follows:

- We propose a flow-guided feature alignment module (FFAM), which utilizes the optical flow between bracket images to guide the deformable alignment module and the spatial attention module, achieving better alignment performance.
- We propose an enhanced feature aggregation module (EFAM), which uses the proposed enhanced residual block (ERB) as its foundational component, enabling more efficient aggregation of inter-frame features.
- We adapt the Bayer preserving augmentation (BayerAug) to raw bracket images for more effective augmentation, allowing the reconstruction of finer details.
- Experimental results demonstrate that the proposed approach achieves better performance than the state-of-the-art methods, both quantitatively and qualitatively.

2. Related Work

Burst Image Restoration and Enhancement Image enhancement and restoration based on burst inputs primarily focus on tasks such as image denoising [14, 26, 32, 39], de-

blurring [1, 10, 37], and super-resolution [2, 3, 6, 24, 25], which utilize the information from multiple consecutive frames with the same exposure to restore the target image. For instance, Godard *et al.* demonstrated that burst inputs provide large improvements over deep learning single-frame denoising techniques [14]. Delbracio *et al.* introduced a fast method for merging a burst of images into a single image, which is both sharper and less noisy than all the images in the burst. Goutam *et al.* recently introduced a method that leverages deep learning networks for burst super-resolution, which takes multiple noisy raw images as input and generates a single RGB image that is both denoised and super-resolved. Although BurstIRE methods have a clear advantage over single-image IRE, they still lack abundant scene information and priors, such as a broader dynamic range and richer levels of noise and motion blur.

Multi-exposure Image Restoration and Enhancement

Multi-exposure-based image enhancement and restoration primarily focus on HDR reconstruction, since images with different exposures can provide distinct details and dynamic range information. Kalantari *et al.* first proposed a CNN-based approach for multi-exposure HDR imaging of dynamic scenes. Subsequently, a lot of CNN-based [22, 28, 30, 31, 38, 40] and Transformer-based [8, 23, 33, 35] methods have been proposed to enhance alignment and fusion performance in multi-exposure HDR reconstruction. Recently, several methods have been proposed that take noise and resolution into account, offering joint HDR reconstruction along with denoising or super-resolution [9, 20, 34]. In this paper, we consider more practical scenarios with severe noise and motion blur and propose a method capable of effectively performing joint HDR reconstruction, denoising, and deblurring.

3. Method

3.1. Overview

As illustrated in Fig. 2(a), the overall pipeline of the proposed IREANet mainly consists of four components, i.e., feature extraction, flow-guided feature alignment, enhanced feature aggregation, and reconstruction.

Given the input bracket multi-exposure images $\{x_i\}_{i=1}^N$ ($x_i \in \mathbb{R}^{4 \times H \times W}$, N is the number of input exposures, H , W is the height and width of the raw image), which are all 4-channels ‘RGGB’ RAW images with noise, blur, and low dynamic range, the task of BracketIRE aims to reconstruct a clear and high dynamic range RAW image $I_H \in \mathbb{R}^{4 \times H \times W}$. In our experiments, we take the shortest-exposure image x_1 as the reference frame x_{ref} and the remaining images as non-reference frames.

3.2. Network Structure

Feature Extraction Given the input images $\{x_i\}_{i=1}^N$, We

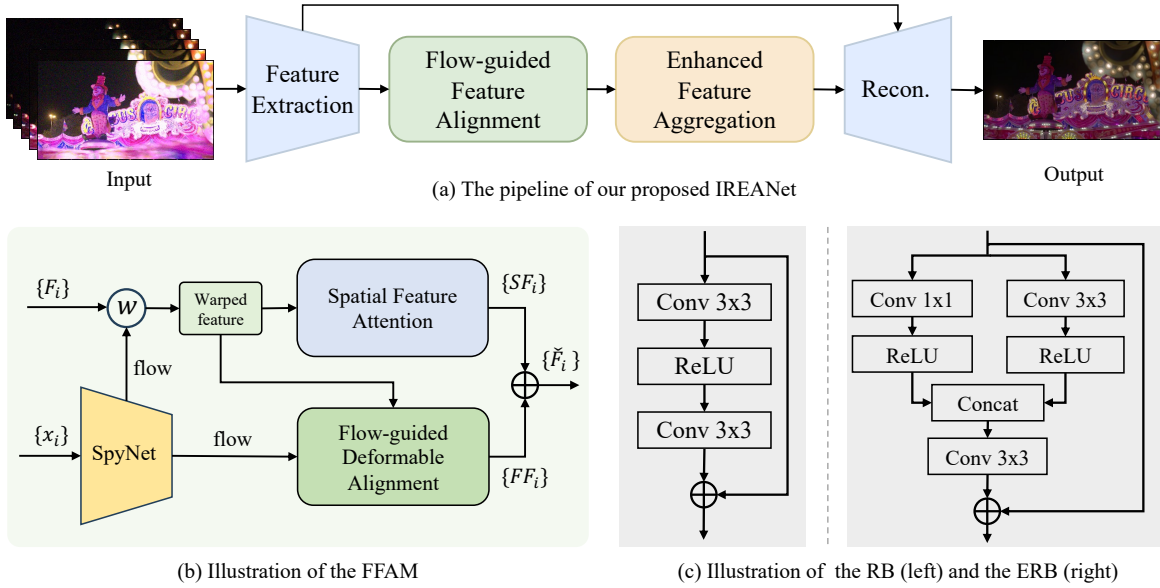


Figure 2. Illustration of the overall framework of the proposed IREANet. As shown in Fig. 2(a), the pipeline mainly consists of four components: feature extraction, feature alignment, feature aggregation, and reconstruction. Fig. 2(b) illustrates the proposed flow-guided feature alignment module (FFAM). Fig. 2(c) depicts the differences between the vanilla residual block (RB) and the proposed enhanced residual block (ERB).

first extract informative features $\{F_i\}_{i=1}^N$ through a feature extraction module, i.e.,

$$\{F_i\}_{i=1}^N = \mathcal{M}_{FE}(\{x_i\}_{i=1}^N). \quad (1)$$

The feature extraction module consists of several residual blocks. In the meanwhile, we send the input images to the SpyNet to obtain the optical flows which are calculated between each no-reference frame $\{x_i\}_{i=2}^N$ and the reference frame x_{ref} :

$$\{f_i\}_{i=2}^N = \mathcal{M}_{SpyNet}(x_i, x_{ref}), i \in 2, 3, \dots, N \quad (2)$$

The non-reference features $\{F_i\}_{i=2}^N$ are then warped by the estimated optical flows, generating the warped features:

$$\hat{F}_i = \mathcal{W}(F_i, f_i), \quad (3)$$

where \mathcal{W} denotes the wrapping operator. More precisely, the \hat{F}_1 is the same as the reference feature.

Flow-guided Feature Alignment Inspired by BasicVSR++ [7] and BSRT [23], we employ the optical flows to guide the feature alignment. Specifically, we propose a flow-guided feature alignment module (FFAM), which is designed as a dual-branch architecture to perform feature alignment. The first branch takes the extracted features and optical flows as input, with the optical flows being considered a rough alignment prior, to guide the DCNs in learning more accurate offsets for flow-guided deformable

alignment (FDA).

$$\{FF_i\}_{i=1}^N = \mathcal{M}_{FDA}(\{F_i\}_{i=1}^N, \{\hat{F}_i\}_{i=1}^N, \{f_i\}_{i=2}^N). \quad (4)$$

The second branch performs spatial feature attention (SFA) on the warped features, obtaining spatial attention features:

$$\{SF_i\}_{i=1}^N = \mathcal{M}_{SFA}(\{\hat{F}_i\}_{i=1}^N). \quad (5)$$

The spatial attention mechanism has been proven to effectively reduce noise and undesired contents caused by foreground object movement [23, 40]. The flow-guided aligned features $\{FF_i\}_{i=1}^N$ and the spatial attention features $\{SF_i\}_{i=1}^N$, serving as complementary features, are then combined through element-wise addition to acquire the final aligned features $\{\tilde{F}_i\}_{i=1}^N$.

Enhanced Feature Aggregation Similar to TMRNet [44], a unidirectional recurrent network is utilized to aggregate temporal features. However, through our experiments, we discovered that the aggregation module using original residual blocks tends to induce training instabilities and fails to converge effectively. Consequently, we introduce an enhanced feature aggregation module (EFAM), which incorporates the proposed enhanced residual block (ERB) as basic components. The proposed ERB increases the network's nonlinearity and enables better convergence, thus allowing for more effective aggregation of informative temporal fea-

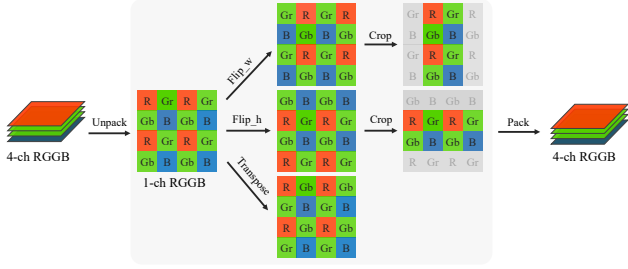


Figure 3. Illustration of the adopted Bayer preserving augmentation (BayerAug).

tures. This process can be formulated as:

$$AF = \mathcal{M}_{EFAM}(\{\tilde{F}_i\}_{i=1}^N). \quad (6)$$

Reconstruction Finally, the aggregated features AF are fed into a reconstruction network composed of several residual blocks, generating the final high-quality HDR result. We also adopt the skip connection to stabilize the training process, i.e.,

$$I_H = \mathcal{M}_{Recon}(AF) + F_1. \quad (7)$$

3.3. Training Strategy

Bayer Preserving Augmentation As demonstrated in [19], employing augmentation methods designed for RGB images on raw images is error-prone. Therefore, we utilize the Bayer preserving augmentation (BayerAug) to augment the training data. The primary process of the BayerAug is shown in Figure 3. As can be seen, a vertical or horizontal flip switches the Bayer pattern from RGGGB to GRBG or GBRG, which may lead to errors during the training process, thereby affecting the details of the reconstruction results. To preserve the correct Bayer pattern during augmentation, we combine flipping and cropping together. Taking vertical flipping as an example, after flipping an image, we apply horizontal cropping to ensure that the Bayer pattern remains correct after augmentation.

Loss Function Inspired by existing methods [17, 23, 40], we compute the loss in the tonemapped domain as HDR images are commonly viewed after tonemapping. We use the μ -law function as the tonemapping operator:

$$\mathcal{T}(x) = \frac{\log(1 + \mu x)}{1 + \mu}, \quad (8)$$

where $\mathcal{T}(x)$ is the tonemapped HDR image. In this paper, we set μ to 5000. In our experiments, we utilize the widely adopted l_1 loss as the loss function, i.e.,

$$\mathcal{L} = \|\mathcal{T}(I_{GT}) - \mathcal{T}(I_H)\|_1, \quad (9)$$

where I_{GT} and I_H denote the ground-truth HDR image and the reconstructed image, respectively.

4. Experiment

4.1. Dataset and Implementation Details

We train and evaluate our method on the Brackett dataset [45] provided by the NTIRE2024 Bracketing Image Restoration and Enhancement Challenge. It contains 1045 scenes in total. We select 100 scenes as the validation set and keep the remaining as the training set. Each scene consists of five LDR images with their corresponding HDR ground truth. Each LDR image contains degradations like ill-exposure, noise, and blur. During the training stage, we first crop the input LDR images to 128×128 patches. We use Bayer pattern augmentation with a random combination of vertical flip, horizontal flip, and rotation. The network is optimized by an AdamW optimizer with a cosine learning rate scheduler. The initial learning rate is 0.0001 and the decay rate is 0.01.

Our experiments are implemented in PyTorch and trained on 4 NVIDIA 2080Ti GPUs with a batch size of 8. We train the model from scratch for 1000 epochs, and the whole training costs about 176 hours. We select the best model using the PSNR score calculated on our validation set when the training reaches plateaus. The entire testing process is conducted on a single Tesla P40 GPU. We test our model with the full-size ($5 \times 4 \times 960 \times 540$) of input, and it takes about 6.1s and 15G memory for each sample. We compute the PSNR, SSIM, and LPIPS scores as the testing metrics with the images on tonemapped domain.

4.2. Results and Analysis

To demonstrate the superiority of our proposed IREANet, we compare it with existing state-of-the-art methods, which include two burst-based methods (i.e., MFIR [4] and Burststomer [12]) and six bracket-based methods (i.e., AHDRNet [40], HDR-GAN [28], CA-ViT [23], SCTNet [35], Kim *et al.* [18], and TMRNet [44]). For fair comparisons, the quantitative results of previous work are borrowed from TMRNet [44] except AHDRNet [40] and CA-ViT [23], which we retrained in the BracketIRE [45] dataset following the same settings as our method to obtain both quantitative and qualitative results.

Quantitative results The quantitative results are listed in Table 1. As can be seen, the proposed IREANet outperforms both the burst-based and bracket-based approaches by a large margin, achieving a 1.59dB gain than the second-best method TMRNet [44].

Qualitative results Fig. 4 illustrates the qualitative results compared with the existing state-of-the-art methods. For each scene, the first row shows the input bracket images, and the second row presents the compared tonemapped results. As shown, in the first scene, the input brackets exhibit ill exposure along with lens flare, making it difficult for recent SOTA methods to recover the texture of the image.

Table 1. Quantitative comparisons of our method with several representative multi-frame IRE methods on the BracketIRE dataset. We report the widely used metrics PSNR, SSIM, and LPIPS.

Method	MFIR [4]	Burstormer [12]	AHDRNet [40]	HDRGAN [28]	CA-ViT [23]	SCTNet [35]	Kim et al. [18]	TMRNet [44]	IREANet Ours
PSNR \uparrow	33.92	37.01	36.32	35.07	36.54	36.90	37.93	38.19	39.78
SSIM \uparrow	0.9026	0.9454	0.9273	0.9157	0.9341	0.9437	0.9452	0.9488	0.9556
LPIPS \downarrow	0.196	0.127	0.154	0.177	0.127	0.120	0.115	0.112	0.102

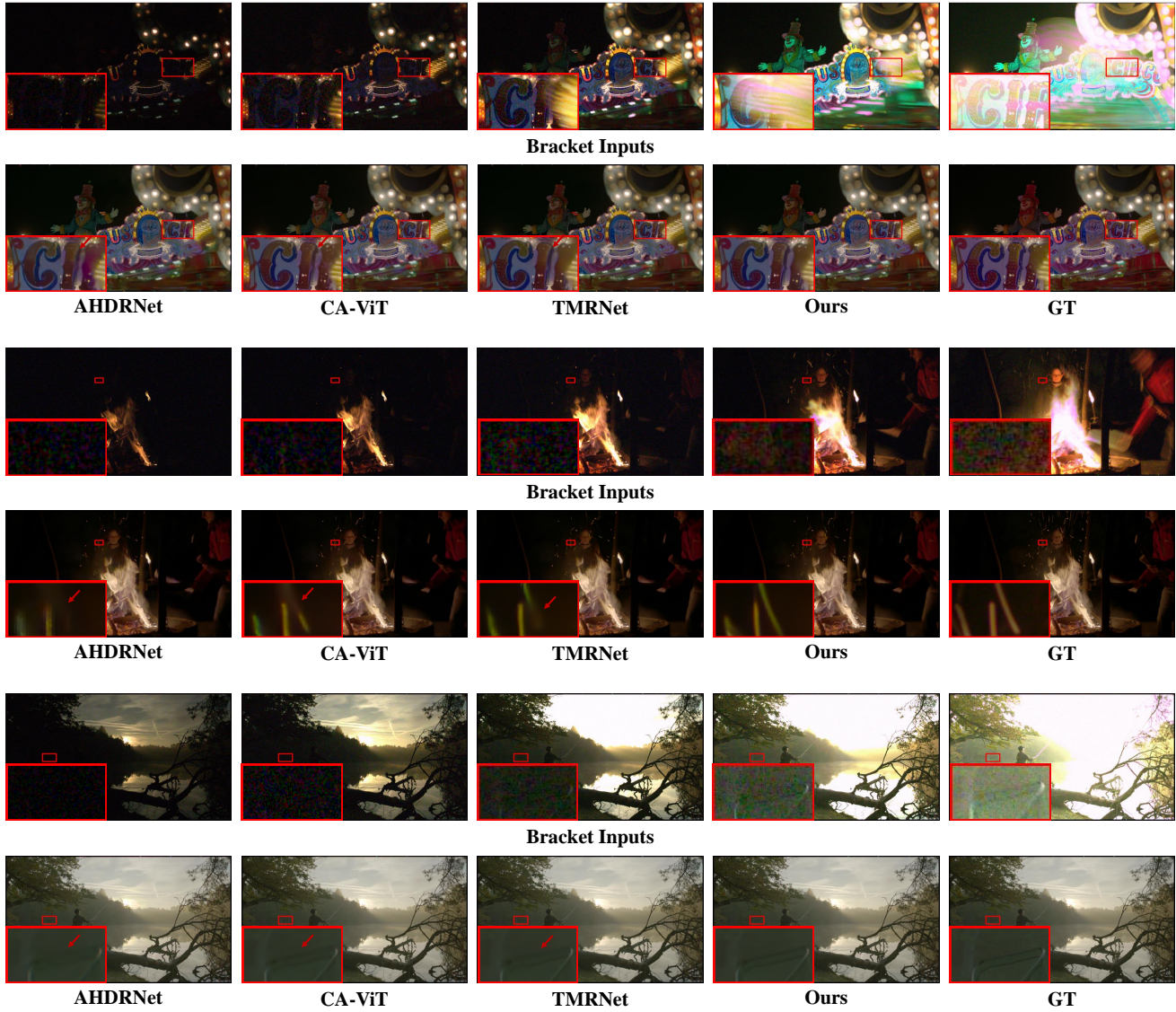


Figure 4. Qualitative Comparison with existing state-of-the-art methods AHDRNet [40], CA-ViT [23], and TMRNet [44]. Our approach can effectively restore high-quality image details from multiple exposure inputs.

In the second and third scenes, the input multi-exposure images suffer from heavy noise and motion blur. These factors cause other methods to encounter issues such as loss of image details and lack of sharpness in these scenes.

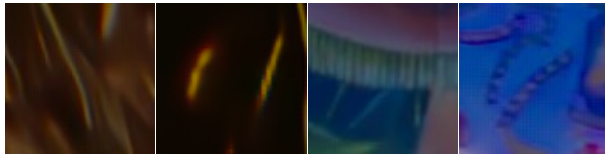
On the contrary, our proposed IREANet reconstructs high-quality HDR results with realistic image details, which further demonstrates the effectiveness of our method.

Table 2. Quantitative results of the ablation studies.

—	Bayer Aug.	EFAM	FFAM	PSNR	SSIM
Baseline				38.19	0.9488
Variant1	✓			39.02	0.9515
Variant2	✓	✓		39.54	0.9541
IREANet	✓	✓	✓	39.78	0.9556



(a) w/o Bayer Aug.



(b) w/ Bayer Aug.

Figure 5. Qualitative results of our ablation study on the Bayer preserve augmentation.

4.3. Ablation Study

To verify the effectiveness of the proposed IREANet, we conduct ablation studies of our contributions and analyze the results on the test set provided by NTIRE2024 Bracketing Image Restoration and Enhancement Challenge. We compare our method with three variants as follows:

- **Baseline.** Our method takes the TMRNet [44] as our baseline, which is one of the SOTA methods in recent BracketIRE works.
- **Variant1.** This variant applies augmentations with random flip and rotation in a Bayer augmentation manner.
- **Variant2.** This variant replaces the basic enhanced residual convolution blocks (ERB) in the backbone of the baseline with our proposed enhanced feature aggregation module (EFAM).
- **IREANet.** The entire network architecture of the proposed IREANet, which contains an enhanced feature aggregation module (EFAM) and flow-guided feature alignment module (FFAM).

As shown in Table 2, variant 1 only applies the Bayer augmentation on TMRNet in the training process. Compared with the baseline model and vanilla augmentation, training with the augmentations in a Bayer augmentation manner shows better performance. The variant1 has a 0.83dB gain of PSNR. The main reason can be concluded that there are differences between data augmentation for Bayer raw images and RGB images. Employing an appropriate image augmentation on bayer raw images can make



Baseline +EFAM +FFAM

Figure 6. Qualitative comparison of our ablation study on the proposed EFAM and FFAM.

the augmented data closer to the real data distribution, leading to an improvement in network training effectiveness. The qualitative comparison results between bayer augmentation and the baseline can be seen in Fig. 5. When we apply the bayer augmentation method on bayer raw images to train the network, the generated images gain richer textures and clearer content.

We also conduct experiments to explore the effectiveness of our proposed module. As shown in Table 2, the variant2 where the ERBs in the network backbone of baseline are replaced with EFAM, showing 0.52dB improvement in PSNR compared to variant1. Additionally, incorporating FFAM on variant 2 gains another 0.24dB improvement, demonstrating the effectiveness of our proposed modules. The qualitative comparison of the ablation experiments on the modules we proposed can be seen in Fig. 6. Employing EFAM on baseline structure obtains richer textures, and further adding FFAM improves the sharpness of image textures, thus validates the conclusion mentioned earlier.

5. Conclusion

In this paper, we have introduced a novel framework (namely IREANet) for the task of Bracket Image Restoration and Enhancement (BracketIRE), which requires utilizing a sequence of noisy, blurred, and low dynamic range multi-exposure RAW inputs to generate high-quality high dynamic range (HDR) images. The model incorporates a Flow-guide Feature Alignment Module (FFAM) and an Enhanced Feature Aggregation Module (EFAM) to improve feature alignment and aggregation. Additionally, we have employed a Bayer-preserving augmentation strategy to improve the generalization capabilities while maintaining the correct Bayer pattern. Experimental results have shown that our IREANet achieves state-of-the-art performance, producing high-quality HDR images with clear content and enhanced details. The proposed method has also achieved second place in the NTIRE 2024 BracketIRE Challenge.

References

- [1] Miika Aittala and Frédo Durand. Burst image deblurring using permutation invariant convolutional neural networks. In *ECCV*, pages 731–747, 2018.
- [2] Goutam Bhat, Martin Danelljan, and Radu Timofte. Ntire 2021 challenge on burst super-resolution: Methods and results. In *CVPRW*, pages 613–626, 2021.
- [3] Goutam Bhat, Martin Danelljan, Luc Van Gool, and Radu Timofte. Deep burst super-resolution. In *CVPR*, pages 9209–9218, 2021.
- [4] Goutam Bhat, Martin Danelljan, Fisher Yu, Luc Van Gool, and Radu Timofte. Deep reparametrization of multi-frame super-resolution and denoising. In *ICCV*, pages 2460–2470, 2021.
- [5] Goutam Bhat, Martin Danelljan, Radu Timofte, Yizhen Cao, Yuntian Cao, Meiya Chen, Xihao Chen, Shen Cheng, Akshay Dudhane, Haoqiang Fan, et al. Ntire 2022 burst super-resolution challenge. In *CVPRW*, pages 1041–1061, 2022.
- [6] Goutam Bhat, Michaël Gharbi, Jiawen Chen, Luc Van Gool, and Zhihao Xia. Self-supervised burst super-resolution. In *ICCV*, pages 10605–10614, 2023.
- [7] Kelvin CK Chan, Shangchen Zhou, Xiangyu Xu, and Chen Change Loy. Basicvsr++: Improving video super-resolution with enhanced propagation and alignment. In *CVPR*, pages 5972–5981, 2022.
- [8] Rufeng Chen, Bolun Zheng, Hua Zhang, Quan Chen, Cheng-gang Yan, Gregory Slabaugh, and Shanxin Yuan. Improving dynamic hdr imaging with fusion transformer. In *AAAI*, pages 340–349, 2023.
- [9] Yiheng Chi, Xingguang Zhang, and Stanley H Chan. Hdr imaging with spatially varying signal-to-noise ratios. In *CVPR*, pages 5724–5734, 2023.
- [10] Mauricio Delbracio and Guillermo Sapiro. Burst deblurring: Removing camera shake through fourier burst accumulation. In *CVPR*, pages 2385–2393, 2015.
- [11] Akshay Dudhane, Syed Waqas Zamir, Salman Khan, Fahad Shahbaz Khan, and Ming-Hsuan Yang. Burst image restoration and enhancement. In *CVPR*, pages 5759–5768, 2022.
- [12] Akshay Dudhane, Syed Waqas Zamir, Salman Khan, Fahad Shahbaz Khan, and Ming-Hsuan Yang. Burstformer: Burst image restoration and enhancement transformer. In *CVPR*, pages 5703–5712. IEEE, 2023.
- [13] Gabriel Eilertsen, Joel Kronander, Gyorgy Denes, Rafal K Mantiuk, and Jonas Unger. Hdr image reconstruction from a single exposure using deep cnns. *ACM TOG*, 36(6):1–15, 2017.
- [14] Clément Godard, Kevin Matzen, and Matt Uyttendaele. Deep burst denoising. In *ECCV*, pages 538–554, 2018.
- [15] Samuel W Hasinoff, Dillon Sharlet, Ryan Geiss, Andrew Adams, Jonathan T Barron, Florian Kainz, Jiawen Chen, and Marc Levoy. Burst photography for high dynamic range and low-light imaging on mobile cameras. *ACM TOG*, 35(6):1–12, 2016.
- [16] Hai Jiang, Ao Luo, Haoqiang Fan, Songchen Han, and Shuaicheng Liu. Low-light image enhancement with wavelet-based diffusion models. *ACM TOG*, 42(6):1–14, 2023.
- [17] Nima Khademi Kalantari and Ravi Ramamoorthi. Deep high dynamic range imaging of dynamic scenes. *ACM TOG*, 36(4):144, 2017.
- [18] Jungwoo Kim and Min H Kim. Joint demosaicing and deghosting of time-varying exposures for single-shot hdr imaging. In *ICCV*, pages 12292–12301, 2023.
- [19] Jiaming Liu, Chi-Hao Wu, Yuzhi Wang, Qin Xu, Yuqian Zhou, Haibin Huang, Chuan Wang, Shaofan Cai, Yifan Ding, Haoqiang Fan, et al. Learning raw image denoising with bayer pattern unification and bayer preserving augmentation. In *CVPRW*, pages 0–0, 2019.
- [20] Shuaizheng Liu, Xindong Zhang, Lingchen Sun, Zhetong Liang, Hui Zeng, and Lei Zhang. Joint hdr denoising and fusion: A real-world mobile hdr image dataset. In *CVPR*, pages 13966–13975, 2023.
- [21] Yu-Lun Liu, Wei-Sheng Lai, Yu-Sheng Chen, Yi-Lung Kao, Ming-Hsuan Yang, Yung-Yu Chuang, and Jia-Bin Huang. Single-image hdr reconstruction by learning to reverse the camera pipeline. In *CVPR*, pages 1651–1660, 2020.
- [22] Zhen Liu, Wenjie Lin, Xinpeng Li, Qing Rao, Ting Jiang, Mingyan Han, Haoqiang Fan, Jian Sun, and Shuaicheng Liu. Adnet: Attention-guided deformable convolutional network for high dynamic range imaging. In *CVPRW*, pages 463–470, 2021.
- [23] Zhen Liu, Yinglong Wang, Bing Zeng, and Shuaicheng Liu. Ghost-free high dynamic range imaging with context-aware transformer. In *ECCV*, pages 344–360. Springer, 2022.
- [24] Ziwei Luo, Lei Yu, Xuan Mo, Youwei Li, Lanpeng Jia, Haoqiang Fan, Jian Sun, and Shuaicheng Liu. Ebsr: Feature enhanced burst super-resolution with deformable alignment. In *CVPRW*, pages 471–478, 2021.
- [25] Ziwei Luo, Youwei Li, Shen Cheng, Lei Yu, Qi Wu, Zhihong Wen, Haoqiang Fan, Jian Sun, and Shuaicheng Liu. Bsrt: Improving burst super-resolution with swin transformer and flow-guided deformable alignment. In *CVPRW*, pages 998–1008, 2022.
- [26] Ben Mildenhall, Jonathan T Barron, Jiawen Chen, Dillon Sharlet, Ren Ng, and Robert Carroll. Burst denoising with kernel prediction networks. In *CVPR*, pages 2502–2510, 2018.
- [27] Seungjun Nah, Tae Hyun Kim, and Kyoung Mu Lee. Deep multi-scale convolutional neural network for dynamic scene deblurring. In *CVPR*, pages 3883–3891, 2017.
- [28] Yuzhen Niu, Jianbin Wu, Wenxi Liu, Wenzhong Guo, and Rynson WH Lau. Hdr-gan: Hdr image reconstruction from multi-exposed ldr images with large motions. *IEEE TIP*, 30: 3885–3896, 2021.
- [29] Eduardo Pérez-Pellitero, Sibi Catley-Chandar, Ales Leonardis, and Radu Timofte. Ntire 2021 challenge on high dynamic range imaging: Dataset, methods and results. In *CVPRW*, pages 691–700, 2021.
- [30] K Ram Prabhakar, Susmit Agrawal, Durgesh Kumar Singh, Balraj Ashwath, and R Venkatesh Babu. Towards practical and efficient high-resolution hdr deghosting with cnn. In *ECCV*, pages 497–513. Springer, 2020.

- [31] K Ram Prabhakar, Gowtham Senthil, Susmit Agrawal, R Venkatesh Babu, and Rama Krishna Sai S Gorthi. Labeled from unlabeled: Exploiting unlabeled data for few-shot deep hdr deghosting. In *CVPR*, pages 4875–4885, 2021.
- [32] Xuejian Rong, Denis Demandolx, Kevin Matzen, Priyam Chatterjee, and Yingli Tian. Burst denoising via temporally shifted wavelet transforms. In *ECCV*, pages 240–256. Springer, 2020.
- [33] Jou Won Song, Ye-In Park, Kyeongbo Kong, Jaeho Kwak, and Suk-Ju Kang. Selective transhdr: Transformer-based selective hdr imaging using ghost region mask. In *ECCV*, pages 288–304. Springer, 2022.
- [34] Xiao Tan, Huaian Chen, Kai Xu, Yi Jin, and Changan Zhu. Deep sr-hdr: Joint learning of super-resolution and high dynamic range imaging for dynamic scenes. *IEEE TMM*, 25: 750–763, 2021.
- [35] Steven Tel, Zongwei Wu, Yulun Zhang, Barthélemy Heyrman, Cédric Démonceaux, Radu Timofte, and Dominique Ginhac. Alignment-free hdr deghosting with semantics consistent transformer. In *ICCV*, 2023.
- [36] Lin Wang and Kuk-Jin Yoon. Deep learning for hdr imaging: State-of-the-art and future trends. *IEEE TPAMI*, 44(12): 8874–8895, 2021.
- [37] Patrick Wieschollek, Bernhard Schölkopf, Hendrik PA Lensch, and Michael Hirsch. End-to-end learning for image burst deblurring. In *ACCV*, pages 35–51. Springer, 2017.
- [38] Shangzhe Wu, Jiarui Xu, Yu-Wing Tai, and Chi-Keung Tang. Deep high dynamic range imaging with large foreground motions. In *ECCV*, pages 117–132, 2018.
- [39] Zhihao Xia, Federico Perazzi, Michaël Gharbi, Kalyan Sunkavalli, and Ayan Chakrabarti. Basis prediction networks for effective burst denoising with large kernels. In *CVPR*, pages 11844–11853, 2020.
- [40] Qingsen Yan, Dong Gong, Qinfeng Shi, Anton van den Hengel, Chunhua Shen, Ian Reid, and Yanning Zhang. Attention-guided network for ghost-free high dynamic range imaging. In *CVPR*, pages 1751–1760, 2019.
- [41] Syed Waqas Zamir, Aditya Arora, Salman Khan, Munawar Hayat, Fahad Shahbaz Khan, Ming-Hsuan Yang, and Ling Shao. Cycleisp: Real image restoration via improved data synthesis. In *CVPR*, pages 2696–2705, 2020.
- [42] Syed Waqas Zamir, Aditya Arora, Salman Khan, Munawar Hayat, Fahad Shahbaz Khan, Ming-Hsuan Yang, and Ling Shao. Multi-stage progressive image restoration. In *CVPR*, pages 14821–14831, 2021.
- [43] Kai Zhang, Wangmeng Zuo, Yunjin Chen, Deyu Meng, and Lei Zhang. Beyond a gaussian denoiser: Residual learning of deep cnn for image denoising. *IEEE TIP*, 26(7):3142–3155, 2017.
- [44] Zhilu Zhang, Shuohao Zhang, Renlong Wu, Zifei Yan, and Wangmeng Zuo. Bracketing is all you need: Unifying image restoration and enhancement tasks with multi-exposure images. *arXiv preprint arXiv:2401.00766*, 2024.
- [45] Zhilu Zhang, Shuohao Zhang, Renlong Wu, Wangmeng Zuo, Radu Timofte, et al. NTIRE 2024 challenge on bracketing image restoration and enhancement: Datasets, methods and results. In *Proceedings of the IEEE/CVF Conference on Computer Vision and Pattern Recognition (CVPR) Workshops*, 2024.
- [46] Yunhao Zou, Chenggang Yan, and Ying Fu. Rawhdr: High dynamic range image reconstruction from a single raw image. In *ICCV*, pages 12334–12344, 2023.